ACERP: Vol. 4, No.1, (Winter 2018) 12-17

Advanced Ceramics Progress

Research Article

Journal Homepage: www.acerp.ir

An Investigation on Milling Method in Reduction of Magnesium Nano-Powder Particles Based on Sustaining Chemical Activity

A.R. Rezaei [a], I. Mobasherpour *[a], S.M.M. Hadavi[b]

[a]Department Ceramics Department, Materials and Energy Research Center (MERC), P.O. Box 31787-316, Karaj, Alborz, Iran.
[b]Department Ceramics Department, Tarbiat Modares University (TMU), Tehran, Iran.

PAPER INFO

Paper history:
Received 18 November 2017
Accepted in revised form 03 March 2018

Keywords:
Magnesium Powder
Ball Milling
Ethylene Glycol
Chemical Resistance

ABSTRACT

Magnesium has been used in aviation industries, automobile manufacturing, electronics and medical engineering due to its unique properties thus far. The main problem in its utilization is the high reactivity of magnesium with oxygen and humidity, which both changes its properties. The surface charge and different density results in difficulties in dispersion stability of the powder in an organic medium. Therefore, numerous methods have been applied to improve the chemical resistance and surface modification of the powder particles. The ball milling process as well as immersion in Ethylene Glycol was used in this study to increase chemical resistance and micro-sized powder dispersion stability in an organic medium. The x-ray powder diffraction analysis was applied to analyze the phase constitutions formed on the powder surface. Scanning electron microscope (SEM) was also utilized to obtain the morphology and the particle size. Moreover, the simultaneous thermal analysis was executed for determining thermal resistance and reactions, which both were measured dispersion stability before and after ball milling process. Results showed a decrease in average particle size from 100 to 7 μm. The chemical resistances and the stabilization increased in organic solvents.

1. INTRODUCTION

Magnesium possesses unique properties that make it a suitable candidate for different applications. Based on the biocompatibility of Magnesium, it is used in several applications including bio engineering, aviation and automobile (because of low weight to strength ratio), and in-situ food preparation (because of exothermic reaction with oxygen). On the other hand, reducing the particle size or grain structure to nano-scale improves these properties [1, 2].

However, different methods have been applied for synthesis of magnesium nano-size powder. Among these methods, the ball milling is used not only for decreasing the particle size but also to improve the physical and mechanical properties due to high-energy collision of the powders with balls and case [5]. The mechanical ball milling is also known as an appropriate method for synthesizing stabilized or semi-stabilized Nano-powders at room temperature. The most noticeable advantage of this synthesizing method is the ability for expansion in industrial scales [6, 7].

*Corresponding Author's Email: Iman.Mobasherpour@gmail.com (I. Mobasherpour)

From the other point of view, magnesium has a high affinity to oxygen even at ambient temperature. Magnesium powder is burn quickly under the atmospheric conditions. Bulk magnesium reacts with oxygen or humidity in the atmosphere and as a result, its surface covers by a relatively protective film of magnesium hydroxide (Eq.1) and magnesium oxide (Eq.2).

$$Mg + 2\,H_2O \rightarrow Mg\,(OH)_2 + H_2 \qquad \text{(Eq. 1)}$$

$$2\,Mg(s) + O_2(g) \rightarrow 2\,MgO(s) \qquad \text{(Eq. 2)}$$

In order to synthesize the magnesium powder, the surface modification techniques should be applied. There are different methods for increasing chemical resistance of the powder surface; hence, the particle stability in the medium, in which there is an active powder, is synthesized. Using neutral atmosphere or even liquefied nitrogen and wet or vacuum ball milling are considered as other applying methods [8, 9]. One of the most efficient methods used for the synthesis of fine-grains of reactive metals is to increase the surface chemical resistance of the powders through their immersion in an organic medium during ball milling process [9, 10].

2. MATERIALS AND METHODS

Magnesium powder (Merck Art No.845042) with a grain size of 100 µm and 99% purity together with ethylene glycol ($C_2H_6O_2$: Merck Art No. 109621) were used to prevent surface oxidization. Both magnesium and ethylene glycol (EG) have been produced by Merck Company. A balance with accuracy of 0.1 mg for weighting, Cambridge stereo scan SEM and D-500 Siemens XRD were used to analyze the morphology and phase constituents, respectively. Powder blends were then subjected to planetary ball mill at room temperature with the following parameters: charge ratio: 30:1 (wt %.); powder mass: 10 g; balls mass : 300 g; ball diameter: 15 mm and 18 mm and vial speed: 310 rpm.

To increase the collision energy in a fixed orbiting speed during ball milling, the balls with different sizes are recommended. The case of the ball mill chamber has been also made from zirconia-based ceramics in order to decrease the contamination and increase the wear resistance.

The milling chamber containing balls, magnesium powder and ethyl glycol was rotated with 310 rpm for 30 hours. Powders were dried in an oven at 75 ° C for 12 hours and crushed to fine powders prior determination of their chemical resistance.

Moreover, powders were heated to the evaporation temperature of ethyl glycol and the magnesium melting point for 3 hours. Thermal gravimetric (TG) and differential thermal analysis (DTA) tests were applied at 23 ° C, 1 atm, 25% humidity at 1000 ° C with heating rate of 5 ° C per minute.

In order to determine the stability of magnesium powders in organic solvents, a 5 cc suspension was prepared by addition of the ethyl glycol to the magnesium powder in a graduated cylinder, which was ultrasonically mixed for about 5 minutes (Fig.1). After some specific periods, the precipitation, supernatant and total volumes were measured.

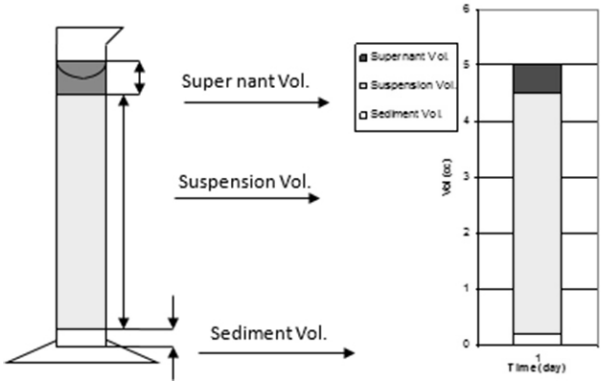

Figure 1. The procedure for reading the amount of supernatant and sediment in the graduated cylinders

3. RESULTS AND DISCUSSION

Fig. 2. shows the XRD pattern of the pure magnesium powder with the average size of 100 µm. The reference magnesium patterns as well as ball-milled powder at 75ºC with average size of 7µm are also shown in Fig. 2. By comparing the XRD patterns, it is evident that the raw magnesium is well matched with the pure magnesium reference patterns, indicating that no oxide or hydroxide has been formed on the surface. The XRD patterns of the ball-milled powders also show that the magnesium oxide or hydroxide has not been formed on the surface of the processed powders. The relatively wide pattern at 32°- to 39º indicates the presence of ethylene glycol as an amorphous phase. It should be mentioned that there is no peak showing any oxide or hydroxide even after drying at 75ºC.

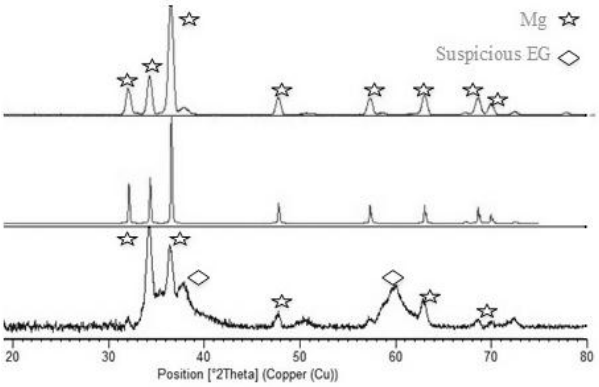

Figure 2. (a) X-ray diffraction of the pure powder magnesium (b) X-ray diffraction of the magnesium reference pattern (c) X-ray diffraction of the ball-milled powder at 75ºC (with a 30:1 weight ratio of ball to powder, 30 hours and 310 rpm as vial speed).

Fig. 3. shows the XRD pattern of the ball-milled magnesium powder sintered in 200ºC and 650ºC. By comparing the pure powder with the one that sintered in 200ºC, we found wide peaks between 32°- to 39º which indicates the presence of amorphous material such as ethylene glycol added as a preventing factor for oxidizing. Therefore, it can be concluded that there is no oxide or hydroxide even after drying at 200ºC. Since there is no wide peak in XRD patterns of the magnesium powders in sintering process at 650ºC, one can conclude that ethylene glycol has evaporated at this temperature.

Based on the XRD pattern of the powders after 30 hours ball milling, it can be said that the presence of ethylene glycol decreases the reactivity, while the uniformity of the powders increases. In fact, a layer from the ethylene glycol covers the surface of the magnesium powder and effectively prevents magnesium oxidation, while the particle size also reduces from 100 to 10 µm. According to the XRD pattern peaks, there is no product formed

based on there action of the magnesium with the ethylene glycol [11-14].

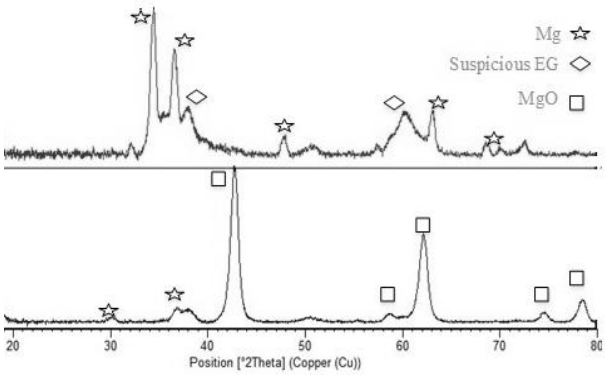

Figure 3. X-ray diffraction pattern (a) milling magnesium powder to ball to powder weight ratio of 30: 1 At the time of 30 hours with 310 rpm and dried at a temperature 75°C (b) X-ray diffraction of the ball-milled powder at 650ºC (with a 30:1 weight ratio of ball to powder, 30 hours and 310 rpm as vial speed)

In order to find out the role of EG in preventing the oxidation of magnesium, the thermodynamic state (Eq. 2) is investigated using Gibbs free energy:

$$\Delta G = \Delta G^{\circ} + RTln\frac{a_{MgO}}{a_{Mg}.P_{O_2}^{1/2}} = \Delta G^{\circ} + RTlnk_p \qquad (\text{Eq. } 3)$$

Because of the equilibrium condition, the equation (3) canbe rewritten as:

$$\Delta G^{\circ} = -RTln\frac{1}{P_{O_2}^{1/2}} = RTlnP_{O_2}^{1/2} \qquad (Eq. 4)$$

According to the information from [13] ΔG° is calculated at 473 K:

$$\Delta G_2^{\circ} = \Delta H° - T\Delta S$$
$$= -608.088 - (11.715TlnT) + (4.602 \times 10^{-3} \times T^2)$$
$$+ \left(5.224 \times \frac{10^5}{T}\right) + 189.844T \qquad (\text{Eq. } 5)$$

$$\Delta H_2^{\circ} = -608.088 + 11.715T - (4.602 \times 10^{-3} \times T^2) + \left(10.447 \times \frac{10^5}{T}\right) \qquad (\text{Eq. } 6)$$

$$\Delta S_2^{\circ} = (11.715lnT) - (9.204 \times 10^{-3}T) + (5.224 \times 10^5/T^2) - 178.129 \qquad (\text{Eq. } 7)$$

By replacing temperature (473°K) in equations 6 and 7, the ΔG° and the oxygen partial pressure can be calculated as:

$$\Delta G_2^{\circ} = -559400\ \frac{\text{J}}{\text{mol}}, \qquad P_{O_2}^{e} = 10^{-134}\ \text{atm}$$

By calculating the Ln k_p from the Vanthof equation (Eq. 8) and replacing number in Eq. 3, the ΔG can be calculated:

$$\frac{\partial lnk_p}{\partial T} = \frac{\Delta H_2^{\circ}}{RT^2} \qquad (\text{Eq. } 8)$$

The $P_{O_2}^{e}$ in Eq. 9 is the oxygen dissociation pressure of magnesium oxide. Based on the oxygen partial pressure at the magnesium/EG interface, there are three different possibilities:

1) if $P_{O_2} < P_{O_2}^{e}$ then oxidation of the metal is not favorable, $\Delta G > 0$

2) if $P_{O_2} > P_{O_2}^{e}$ then the oxidation of magnesium may occur, , $\Delta G < 0$

3) if $P_{O_2} = P_{O_2}^{e}$ then the ΔG is equal to zero and the oxidation process is at equilibrium with the reduction process, $\Delta G = 0$

So, the oxygen dissociation pressure of the magnesium oxide at 200℃ temperature is about 10^{-134} atm. The lack of forming magnesium oxide on its powder indicates that the oxygen partial pressure at the magnesium/EG interface is less than 10^{-134} atm. According to the Ellingham diagram [13], finding out an oxygen dissociation pressure close to what has been calculated, also confirms this situation.

Fig. 4(a) shows the morphology and particle size of the Mg before milling. In general, the milling process has three mechanisms including plastic deformation, fracture and cold welding, which dominates the particle morphology variations [15]. All of them occur in three stages, but the predominance of each mechanism over another lead to the modification of the particles morphology. As seen in Fig. 4(a), the magnesium powder morphology is quasi-spherical with the particle size of 100 micrometers.

Fig. 4(b) shows the sample morphology containing Mg and EG after 30 hours milling. As can be seen in Fig. 4(b), after 30 hours milling, the particle size decreases with deformation along with the welding particles resulting in a wide range of particle sizes shown in Figs. 4(b) and (c).

By comparing Fig.4 (a) and 4 (b), it is evident that the particle size has been reduced to about 10 μm. Then, because of hardening based on plastic deformation of the particles, particles tend to break during milling by hammer hitting of balls. The main failure mechanisms in cold welding are clearly visible in Figs. 4(b) and 4(c). In the milling process, plastic deformation results in increasing dislocation density where sub-boundaries arise, as through continuing the process of milling, the boundaries open borders in order to form large angles. This process is shown in Fig.5 [15]. The balance between cold welding of the fine particles and fracture of the larger particles determines the average size.

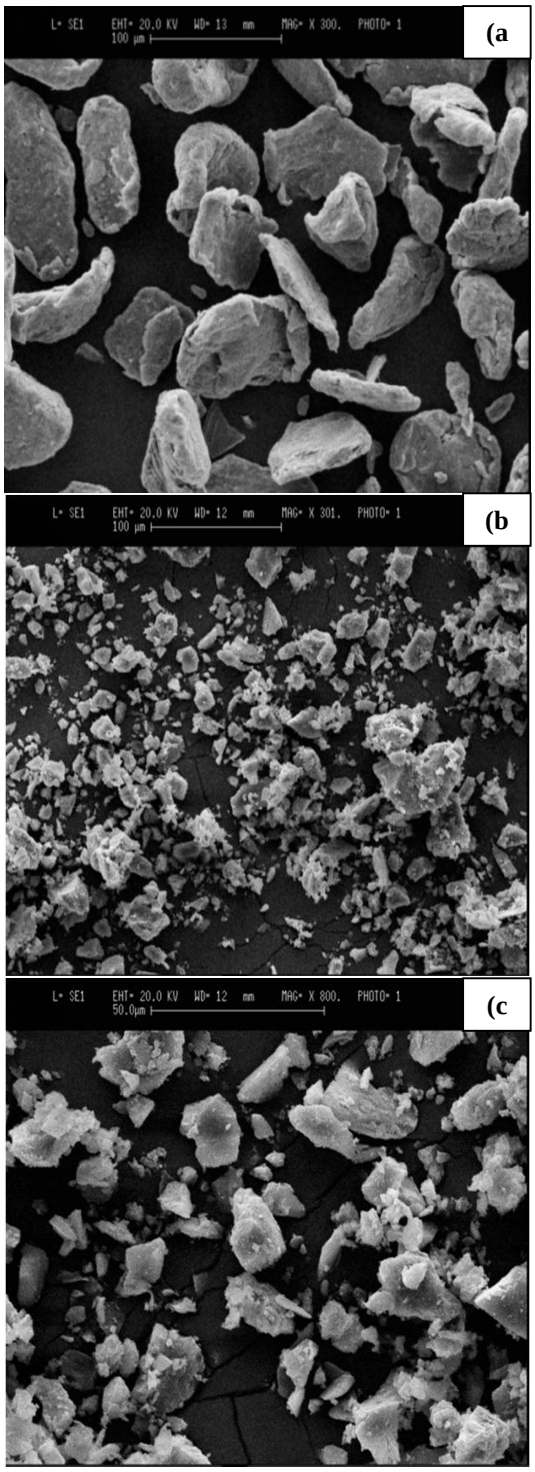

Figure 4. (a) SEM image of pure magnesium powder (b) and (c) SEM images of the ball-milled powder at 75ºC (with a 30:1 weight ratio of ball to powder, 30 hours and 310 rpm as vial speed

Occasionally, a high temperature annealing treatment is needed to obtain the desired structure, especially in the formation time of the desired intermetallic compounds. The time required to achieve the desired structure in any system is a function of the particle size and the behavior of its components [15]. The synthesized crystals size can be identified via two methods. The first is Scherrer method based on the Eq.9:

$$D = \frac{0.9\lambda}{b\ cos\theta} \qquad \text{(Eq. 9)}$$

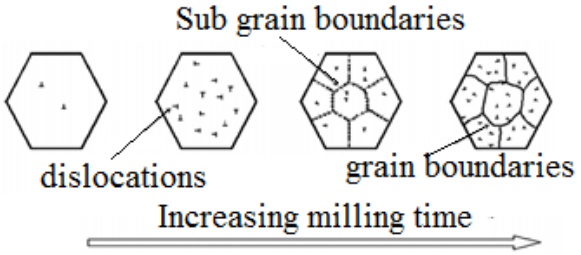

Figure 5. The process of fine-grained structure during the milling process [15]

Where b denotes peak width at half height (in radian), λ is the X-ray wavelength, θ is the diffraction angle of the tallest peak (in radian) and D is the average diameter of the crystal.
The second method is Williamson–Hall in which the strain can be calculated as shown in Eq. (10):

$$b\ cos\theta = \frac{0.9\lambda}{D} + 2\eta\ \sin\theta \qquad \text{(Eq. 10)}$$

Where η is the average strain in the system. By plotting "bcosθ" versus "2sinθ", the line slope represents the strain whereas the intercept shows the average grain size.
Table 1 indicates the average size of the crystals and the strain average for the powder mill powders were calculated by Williamson - Hall method. As the results show, the average crystal size decreases by milling time. In fact, working at the temperatures up to 200ºC does not change the crystal sizes, whereas heating at 650ºC lead to destroying the protective layer and consequently formation of MgO.

TABLE 1. Average size of the crystals and average strain for milled powders calculated by Williamson-Hall method

The average strain	The average size of the crystals (nm)	heated Temperature (℃)	Milling time (hours)
0.63	Mg:5	25	0
0.90	Mg:2	75	30
0.59	Mg:2	200	30
0.03	MgO:15	650	30

Fig. 6. illustrates a result of STA experiment with its first derivative of DTA curve in Fig. 7.for the magnesium powders. As can be seen, the curve's fluctuations reflect the phase changes in the sample. From the oxidation of magnesium powder, it is expected that a continuous mass gain occurs until the melting temperature of the powders. Nevertheless, according to the TG graph, weight loss starts from temperature as low as 180°C. At temperature of about 500°C, an exothermic peak was observed. As the TG graph shows, at this temperature almost 50% weight loss happens. It can be deducted that the weight loss is due to the thermal decomposition of ethylene glycol. Increasing the thermal stability of magnesium powders using ball milling with ethylene glycol, shows that it covers the magnesium powder surface.

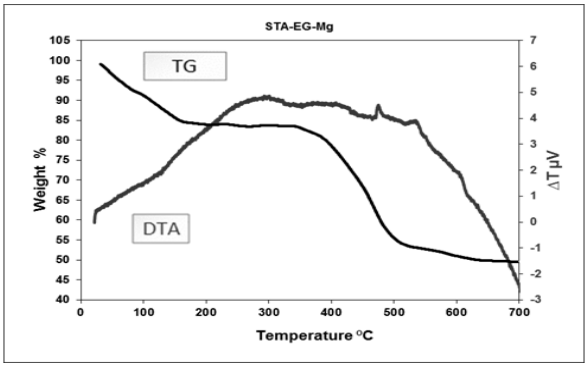

Figure 6. STA experiment of the Magnesium powder milling with ethylene glycol (environmental conditions: temperature at 25 ° C under atmospheric pressure, humidity 25% at a rate of 5°/min)

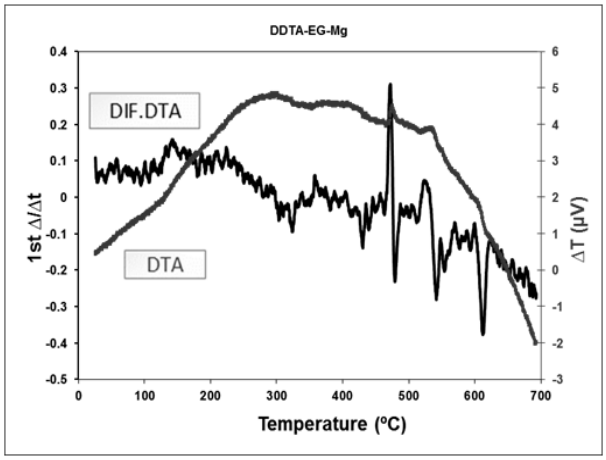

Figure 7. dif. DTA Magnesium powder milling with ethylene glycol (Environmental conditions at 25 ° C under atmospheric pressure humidity 25% at a rate of 5°/min)

The results related to the thermal analysis of samples showed that this technique increases the magnesium thermal stability at 200°C. The magnesium oxidation beyond this temperature causes a relatively high amount of mass gain. As can be seen in TG diagram, with continuing heating process, an endothermic reaction appears due to the magnesium melting process [16, 17].

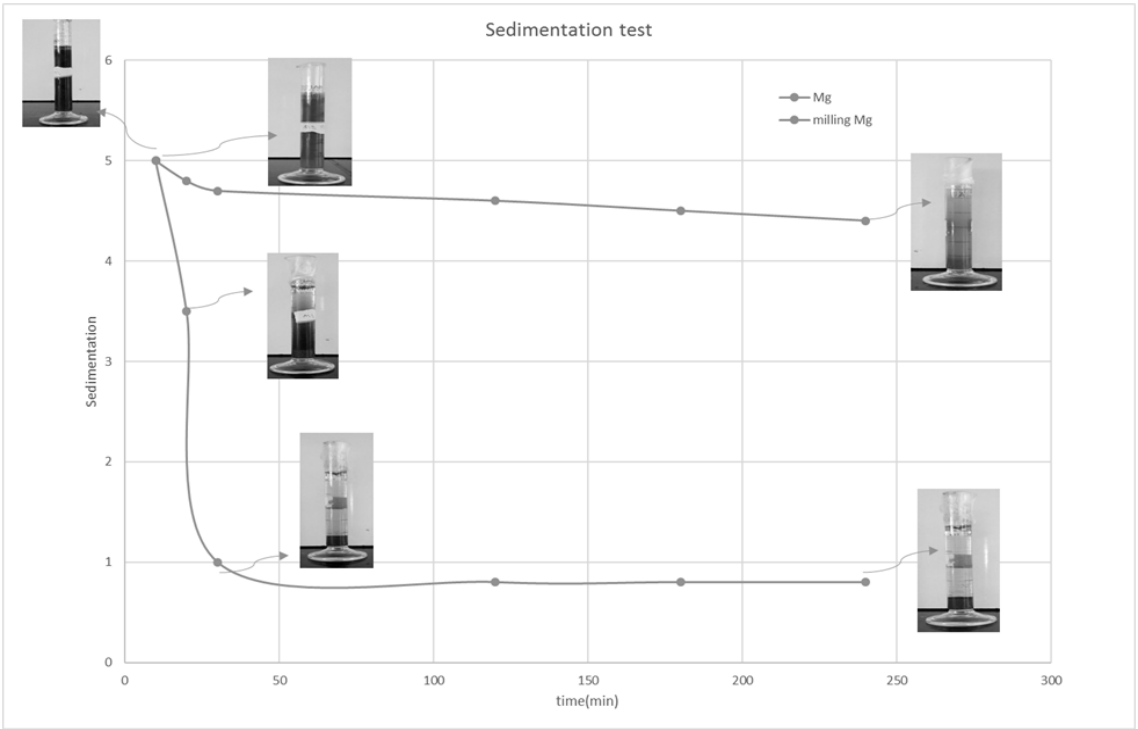

Figure 8. The results of sedimentation test for (a) pure magnesium and (b)magnesium wet ball-milled in ethylene glycol.

The magnesium particle movement is uniform and faster in a stable suspension than an unstable one. In order to have a stable suspension, dispersant materials are used. The other way to have such a suspension media can be acquired by making space prevention using ethylene glycol. Fig. 8, shows the Sediment height with time for pure magnesium as well as magnesium wet ball-milled in ethylene glycol. As can be seen, sediment height decreased 5cmto 1cm in 30 min and5 cm to 4.5cm in 240 min for pure magnesium, and magnesium wet ball-milled in ethylene glycol, correspondingly. Whereas the magnesium seed size decreases and a layer of ethylene glycol creates on the magnesium surface, the weight force as an important factor in precipitation reduces and the space prevention created by the ethylene glycol highly postpones the magnesium precipitation.

4. CONCLUSION

1. In order to prevent the oxidation of magnesium powder during milling, ethylene glycol was used to cover the powder surface.
2. The ball milling of magnesium powder in the ethylene glycol media not only prevents the powder sticking to the balls and the case but also increases the process efficiency.
3. Nanostructured magnesium powder was obtained usingball milling method in the ethylene glycol media without side-reactions or explosion

5. ACKNOWLEDGMENTS

This research was completely supported by Materials and Energy Research Center (MERC) under the student project and will be grateful

REFERENCES

1. Conceicao, T.F., Scharnagl N., Blawert C., Dietzel W., Kainer K.U., *Corrosion Science*, Vol. 52, (2010), 2066-2079.
2. Bridge, D. R., Holland, D. and McMillan, P. W., "Development of alpha-cordierite phase in glass ceramic for use in electronic devices", ***Glass Technology,*** Vol. 26, No. 6, (1985), 286–292.
3. Mussler, B. H. and Shafer, M. W., "Preparation and properties of mullite-cordierite composites", ***Ceramic Bulletin,*** Vol. 63, No. 5, (1984), 705–710.
4. Tummala, R. R., "Ceramic and glass-ceramic packaging in the 1990s", ***Journal of American Ceramic Society,*** Vol. 74, No. 5, (1991), 895–908.
5. Knickerbocker, S. H., Kumar, A. H. and Herron, L. W., "Cordierite glass-ceramics for multilayer ceramic packaging", ***American Ceramic Society Bulletin,*** Vol. 72, No.1, (1993), 90-95.
6. Dupon, R.W., McConville, R.L., Musolf, D.J., Tanous, A.C. and Thompson M.S., "Preparation of cordierite below 1000ºC via bismuth oxide flux", ***Journal of American Ceramic Society,*** Vol. 73, (1990), 335–339.
7. Malachevsky, M.T., Fiscina, J.E. and Esparza, D.A., "Preparation of synthetic cordierite by solid-state reaction via bismuth oxide flux", ***Journal of American Ceramic Society,*** Vol. 84, No. 7, (2001), 1575–1577.
8. Yang, S., Mei, J. and Ferreira J.M.F., "Microstructural evolution in sol–gel derived P2O5-doped cordierite powders", ***Journal of European Ceramic Society,*** Vol. 20, (2000), 2191–2197.
9. Sumi, K., Kobayashi, Y. and Kato, E., "Low-temperature fabrication of cordierite ceramics from kaolinite and magnesium hydroxide with boron oxide additions", ***Journal of American Ceramic Society,*** Vol. 82, No. 3, (1999), 783–785.
10. Suzuki, H., Ota, K. and Saito, H., "Preparation of cordierite ceramics from metal alkoxides", ***Journal of Ceramic Society,*** Vol. 95, (1987), 163–169.
11. Kazakos, A.M., Komarneni, S. and Roy, R., "Sol–gel processing of cordierite: effect of seeding and optimization of heat treatment", ***Journal of Material Research,*** Vol. 5, (1990), 1095–1103.
12. Sumi, K., Kobayashi, Y. and Kato, E., "Synthesis and sintering of cordierite from ultrafine particles of magnesium hydroxide and kaolinite", ***Journal of American Ceramic Society,*** Vol. 81, No. 4, (1998), 1029–1032.
13. Ianos, R., Lazau, I. and Pacurariu C., "Solution combustion synthesis of a-cordierite", ***Journal of Alloys and Compound,*** Vol. 480, (2009), 702–705.
14. Goren, R., Gocmez, H. and Ozgur, C., "Synthesis of cordierite powder from talc, diatomite and alumina", ***Ceramic International,*** Vol. 32, No. 4, (2006), 407–409.
15. Ghitulica, C., Andronescu, E., Nicola, O., Dicea, A. and Birsan, M., "Preparation and characterization of cordierite powders", ***Journal of European Ceramic Society,*** Vol. 27, (2007), 711–713.
16. Oghbaei, M. and Mirzaee, O., "Microwave versus conventional sintering: A review of fundamentals, advantages and applications", ***Journal of Alloys and Compound,*** Vol. 494, (2010), 175–189.
17. Ebadzadeh, T., Sarrafi, M.H. and Salahi, E., "Microwave-assisted synthesis and sintering of mullite", ***Ceramic International,*** Vol. 35, (2009), 3175–3179.
18. Santos, T., Valente, M.A., Monteiro, J., Sousa, J. and Costa, L.C., "Electromagnetic and thermal history during microwave heating", ***Applied Thermal Engineering,*** Vol. 31, No. 16, (2011), 3255–3261.
19. Willert-Porada, M., Grosse-Berg, J., Sen I. and Park H.S., "Microwave sintering and infiltration of highly porous silicon nitride ceramics to form dense ceramics", ***Advance Si-based Ceramic Composites***, Vol. 287, (2005), 171–176.
20. Ebadzadeh, T., "Effect of mechanical activation and microwave heating on synthesis and sintering of nano-structured mullite", ***Journal of Alloys and Compound,*** Vol. 489, No. 1, (2010), 125–129.
21. Kiany, M. and Ebadzadeh, T., "Effect of mechanical activation and microwave sintering on crystallization and mechanical strength of cordierite nanograins", ***Ceramic International,*** Vol. 41, No. 2, (2015), 2342–2347.